Controlling cyclic combustion timing variations using a symbol-statistics predictive approach in an HCCI Engine

Ahmad Ghazimirsaied, Charles Robert Koch*

Department of Mechanical Engineering, University of Alberta, Edmonton, Alberta T6G 2G8, Canada

Abstract

Cyclic variation of a Homogeneous Charge Compression Ignition (HCCI) engine near misfire is analyzed using chaotic theory methods and feedback control is used to stabilize high cyclic variations. Variation of consecutive cycles of θ_{Pmax} (the crank angle of maximum cylinder pressure over an engine cycle) for a primary reference fuel engine is analyzed near misfire operation for five test points with similar conditions but different octane numbers. The return map of the time series of θ_{Pmax} at each combustion cycle reveals the deterministic and random portions of the dynamics near misfire for this HCCI engine. A symbol-statistic approach is used to predict θ_{Pmax} one cycle-ahead. Predicted θ_{Pmax} has similar dynamical behavior to the experimental measurements. Based on this cycle ahead prediction, and using fuel octane as the input, feedback control is used to stabilize the instability of θ_{Pmax} variations at this engine condition near misfire.

Keywords: HCCI, Nonlinear dynamics, Prediction, Control, Symbol-sequence approach

Nomenclature

aBDC	after Bottom Dead Center
aTDC	after Top Dead Center
CAS	Combustion Analysis System
CA50	Crank Angle for 50% mass fraction burnt fuel
θ_{Pmax}	Crank Angle where the maximum pressure inside cylinder occurs
COV	Coefficient of Variation
ECU	Engine Control Unit
EGR	Exhaust Gas Recirculation
EVO	Exhaust Valve Opening
HCCI	Homogeneous Charge Compression Ignition
HR	Heat Release
IMEP	Indicated Mean Effective Pressure
IVC	Intake Valve Closing
Pman	Intake Manifold Pressure
PRF	Primary Reference Fuels - volume percentage of iso-octane in n-heptane

*Corresponding author. Tel: +1 780 492 8821; Fax: +1 780 492 2200.
Email address: bob.koch@ualberta.ca (Charles Robert Koch)

RPM	Revolution Per Minute
SI	Spark Ignition
SOC	Start of Combustion
TDC	Top Dead Center
Tman	Intake Manifold Temperature
Toil	Oil Temperature

1. Introduction

HCCI engines are of interest due to certain advantages over conventional Spark Ignition (SI) and Compression Ignition (CI) engines. In particular, low emission levels in terms of NOx and particulate matter and high thermal efficiency of these engines are beneficial [1]. Two main concerns about this engine technology are: limited operation range, and lack of any direct control on ignition timing [2]. Typically the HCCI operating range is limited by engine damaging knock at high load, and by undesirable high cyclic variation at low load. This paper focuses on understanding how to extending the low load range of HCCI where high cyclic variations are responsible for unstable combustion which limits the operating range of the engine [3]. The combustion stability of a SI engine has been investigated by means of both experimental tests and numerical analysis [4]. Cyclic variations are classified as linear random or having deterministic coupling between consecutive cycles, both of which have been analyzed using nonlinear and chaotic theory [5, 6, 7]. The term deterministic is used when future states, for some horizon of the system, can be calculated from the past values [8]. Temporal dynamics of the combustion process in a lean-burn natural gas engine was studied by the analysis of time series of consecutive experimental in-cylinder pressure data [9, 10]. This structure is then used to predict future cycles and incorporated in a control algorithm to influence the HCCI ignition timing [11, 12]. Thus, understanding the dynamics of HCCI combustion during high cyclic variation operating conditions, could be used to extend the operating range if there is deterministic structure inherent between engine cycles.

Cyclic variation of HCCI is highly dependent on the timing of Start Of Combustion (SOC). Early combustion timing right after Top Dead Center (TDC) tends to have low SOC cyclic variation while late HCCI combustion timing tends to have high cyclic variations [3]. Period-doubling and bifurcation in experimental measurements of SI engines are investigated as the mixture is made leaner [13, 14]. Their results indicate that there is a transition from stochastic behavior to a noisy nonlinear deterministic structure as the mixture is made leaner. This seems to indicate that for lean mixture conditions, cycles are related. Engine dynamics appeared to pass through distinct stages including stochastic, periodic, and chaotic behavior. The combustion process in a SI engine is analyzed and shows that the system can be driven to chaotic behavior [15]. In [16, 17], a method is proposed based on a symbolic approach to measure temporal irreversibility in the time series and a method is introduced to detect and quantify the time irreversibility. In [18], the symbolic method is analyzed such that the symbolization is used to enhance the signal-to-noise ratio. The onset of combustion instabilities under lean mixture conditions have been studied using symbolic methods for observed in-cylinder pressure measurements in SI engines [16, 19]. A time-series analysis technique called symbolic time series analysis is summarized in [20]. The observation of time irreversibility in cycle-resolved combustion measurements of SI engines is discussed

in [11] and the advantage of their model compared to linear gaussian random processes is presented. The transition dynamics from conventional SI combustion to HCCI combustion is described using nonlinear tools in [21], where the cyclic combustion oscillations occurring in transition between the SI and HCCI mode are presented as a sequence of bifurcations in a low-dimensional map. Temporal dynamics of the variation of consecutive cycles of crank angle of 50% mass fraction of fuel burnt (CA50) is analyzed using chaotic theory tools in [22]. The sequential unstable cyclic combustion measurements in the SI-HCCI transition are used to obtain the global kinetic parameters [23]. This aids in discriminating between the multiple combustion states and to provide qualitative insight into the SI-HCCI mode transition. CA50 is predicted one cycle ahead using a symbol-statistics approach in [22].

Fuel stratification have been applied to extend HCCI high load range by controlling the combustion phasing [24]. A parametric study has been performed in order to gain more understanding in the emission reduction possibilities via HCCI new combustion technology [25]. The comparison of the results obtained from a modified HCCI multi-zone model to experimental measurements, at different load and boost pressure conditions are presented in [26]. The possibility of controlling combustion phasing and combustion duration using various Exhaust Gas Recirculation (EGR) fractions have been investigated in [27]. The combustion and emission characteristics of a HCCI engine fueled with ethanol were investigated on a modified two-cylinder, four-stroke engine using port injection technique for preparing homogeneous charge [28]. The implementation of HCCI combustion in direct injection diesel engines using early, multiple and late injection strategies has been reviewed in [29]. The development and a preliminary validation of a heat transfer model for the estimation of wall heat flux in HCCI engines via multi-zone modeling has been the focus of [30]. A multi-zone model is used for the purpose of investigating the importance of mass transfer on the formation of the most important HCCI engine emissions in [31].

The main objective of this paper is to investigate and control the cyclic variation of combustion timing near the misfire limit by using the identified dynamics to predict one cycle ahead and use this prediction in feedback control to stabilize unstable HCCI operation near misfire. Nonlinear and chaotic theory tools are used to identify the inherent deterministic patterns of cyclic variation during HCCI combustion. This paper is organized into sections with the engine experimental procedure described first. Then return maps are used to qualitatively observe the dynamical patterns near engine misfire. The return maps are a useful tool to recognize the dependency of the current combustion cycle on previous ones. Then the deterministic structure inherent in the cyclic engine data at 5 octane numbers is captured using a symbol-sequence approach. Joint probability distributions are calculated from the frequency histograms. Then, a joint probability estimator is used to predict combustion timing one cycle ahead for each octane number. Finally, the cycle ahead prediction at all 5 octane numbers is combined with feedback control that modulates the octane number to control ignition timing and extending the HCCI operating range of the engine.

2. Experimental Procedure and Ignition Timing

The experimental single cylinder engine operating in HCCI mode is detailed in [22]. A schematic of the Ricardo Hydra Mark 3 single cylinder engine fitted with a modified Mercedes E550 cylinder head is shown in Figure 1. This cylinder head is typical for a modern

spark ignition engine with four valves per cylinder and a pent-roof combustion chamber shape. The fuels that are used in this work are blends of n-Heptane and iso-Octane. These two fuels (n-Heptane and iso-Octane) are Primary Reference Fuels for octane rating in internal combustion engines, and have octane number of 0 (100% n-Heptane) and 100 (100% iso-Octane), with cetane number of approximately 56 and 15, which is very similar to the cetane number of conventional gasoline and diesel fuel, respectively. Dual fuel of iso-octane and n-heptane are injected at the intake port of the engine. The fuel is injected into the intake air directly onto the intake valves, at TDC. Both the iso-Octane and n-Heptane injectors are placed at the same distance from the intake valves. These two independent fuel systems are installed on this engine so that blending of iso-Octane and n-Heptane can be done on a real time basis. Port fuel injection is typical of a SI production engine in a modern automobile. Both fuel systems are calibrated to determine the injector flow rates. This is done so that the mass flow rate of both fuels can be estimated. The fuel injection is done with a dSpace-MicroAutobox ECU (Engine Control Unit), which provides accurate control of the injection timing as well as the duration. This ECU also controls the spark timing, which is used during the engine warm up in SI mode but is turned off for HCCI combustion.

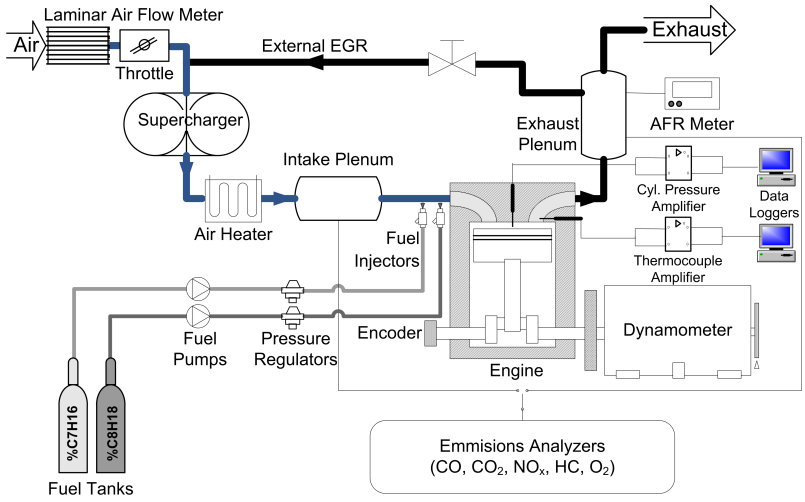

Figure 1: Ricardo single cylinder testbench schematic.

The engine specifications are listed in Table 1. Cylinder pressure is recorded 3600 times per crank revolution and processed with an NI Labview and A&D Baseline CAS using a degree based real time processor. The pressure trace is then analyzed for combustion metrics, such as IMEP and θ_{Pmax}. These metrics are then logged for a duration of 3000 engine cycles.

The details of the base engine experimental conditions used in this study are listed in Table 2.

Table 1: Fixed parameters of the Ricardo single-cylinder engine for the 5 tests

Parameters	Values
Number of Cylinders	1
Bore × stroke [mm]	97 × 88.9
Compression Ratio	12
Displacement [L]	0.653
Connecting rod length [mm]	159
Valves	4
Valve Lift [mm]	9.3

Table 2: Base test operating conditions

Parameters	Values
Engine Speed [RPM]	1000
Manifold Temperature [°C]	38
Oil Temperature [°C]	60
Manifold Pressure [kPa]	93-95
IVC [aBDC]	200
EVC [aBDC]	-26
PRF	3, 4, 5, 6 , 7

θ_{Pmax} is defined as the crank angle of the maximum in-cylinder pressure trace over one engine cycle and is a measure of combustion timing. Using heat release analysis the cyclic variability in ignition timing, θ_{Pmax}, is found to be a robust criteria of ignition timing [32] since θ_{Pmax} depends predominantly on the timing of combustion and is independent of charge variations. This makes it a useful measure of variability in combustion timing [33]. An example of the location of θ_{Pmax} for HCCI combustion is shown in Figure 2 where cylinder pressure is plotted versus crankangle.

3. Cycle-Ahead Prediction

θ_{Pmax} is used as the feedback parameter in this work as it is a simple ignition timing parameter requiring a low amount of computation [34]. A one step ahead prediction of θ_{Pmax}, using previous and current values of θ_{Pmax} is used in subsequent feedback control. To obtain an accurate prediction several techniques are evaluated. First a chaotic analysis is performed on 5 test points with 5 different octane numbers at steady-state for 3000 consecutive engine cycles. Then the data is analyzed at each of these operating points to find the probabilistic histogram. At each of the 5 operating points one set of data is used for analysis while the other set of data is kept for validation. A test point with varying octane number, close to misfire with many partial burn combustion events and with engine torque only slightly above the motoring condition is used as a final validation and is not used to parameterize the model. This is also the condition where feedback control is used to stabilize ignition timing. A flowchart of cycle-ahead prediction based on chaotic analysis results is illustrated in Figure 3. This figure outlines the analysis procedure that is described next.

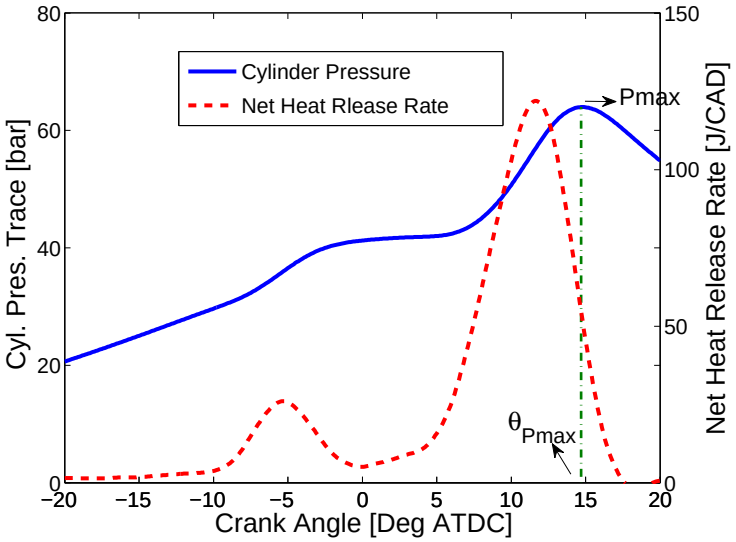

Figure 2: Sample operating point for HCCI combustion

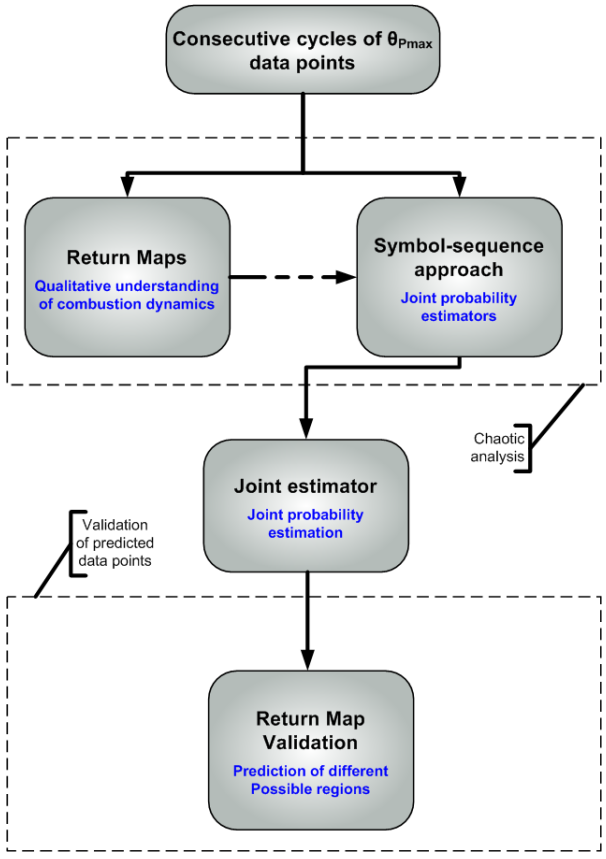

Figure 3: Flowchart: Use of chaotic tools for nonlinear prediction

3.1. Return Maps

A return map can be used to observe the structure inherent in a time series [21]. Here they provide a tool to check the probable interaction between the combustion timing at the current cycle (θ_{Pmax_i}) with the next consecutive cycle ($\theta_{Pmax_{i+1}}$). For a random time series, consecutive cycles are uncorrelated and the return map shows an unstructured cloud of data points gathered around a fixed point. With deterministic coupling between consecutive points, the return map shows more structure such as dispersed data points about a diagonal line [35]. In this paper the analysis of HCCI engine data at condition listed in Table 2 is performed. The octane number is varied from 3 to 7 in steps of 1 by changing the ratio of fuels injected by two fuel injectors and the return maps of all 3000 engine cycles of θ_{Pmax} for these 5 engine operating conditions are shown in Figure 4. The combustion timing return map is a phase plane and plots θ_{Pmax} at cycle $i+1$ on the y-axis and θ_{Pmax} at cycle i on the x-axis where i represents the cycle (time).

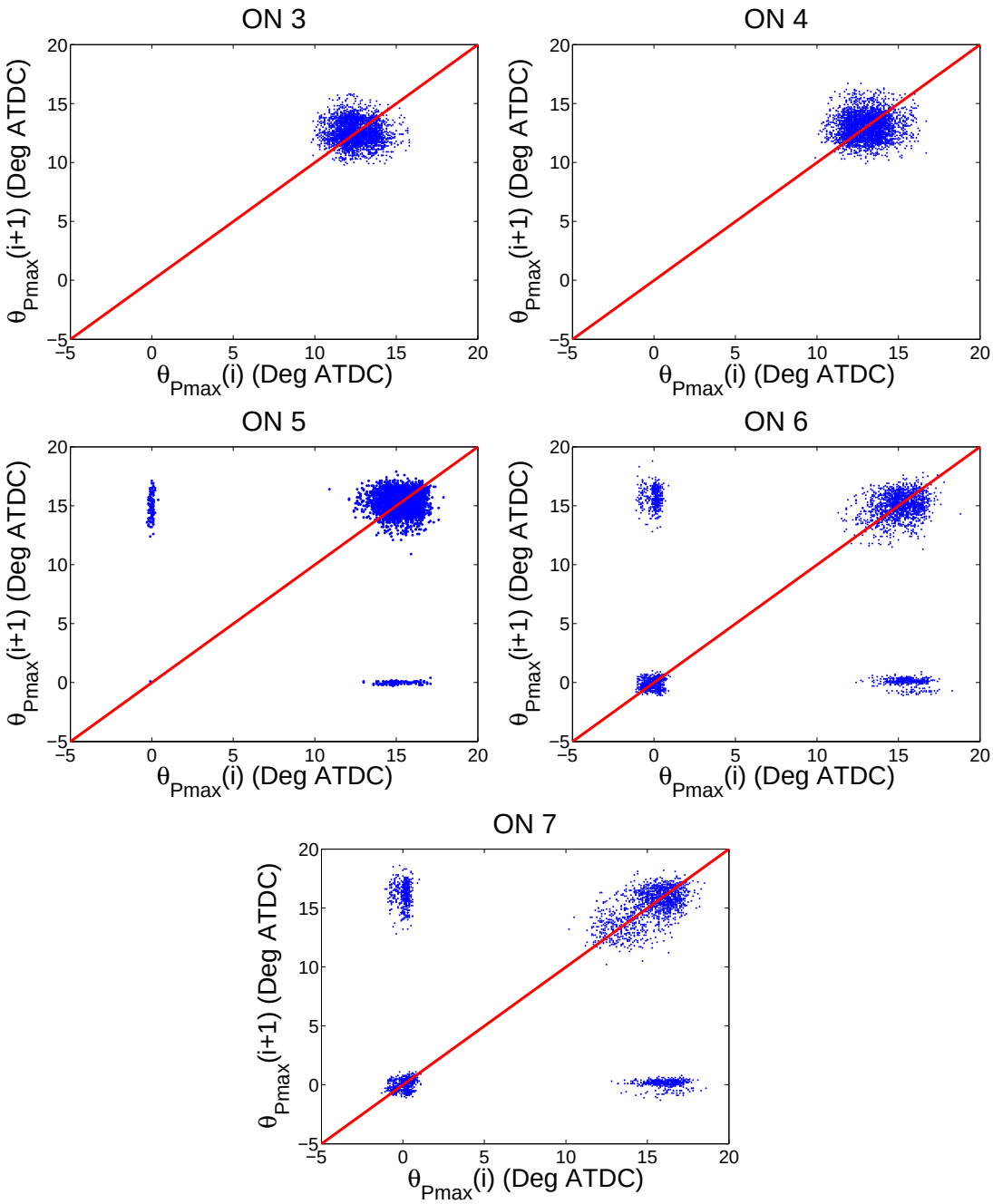

Figure 4: Return map of combustion timing, θ_{Pmax}, for 5 octane numbers. conditions listed in Table 2

The relationship between combustion timing of the current cycle and the next cycle indicates that for some of the cases shown in Figure 4 there is a deterministic dependency on previous cycles. In these cases, predicting future cycles (for some prediction horizon) using previous combustion cycles is possible. However, the detailed relationship between cycles is not apparent in Figure 4 and further analysis is needed. To characterize the combustion timing dynamics, the following functional form for θ_{Pmax} (at cycle i) using previous cycles

is used:

$$\theta_{Pmax}(i) = f(\theta_{Pmax}(i-1), \theta_{Pmax}(i-2), ..., \theta_{Pmax}(i-(L-1)))$$

Chaotic tools such as return maps and symbol-sequence techniques are used to find the approximate function f and value of L. Since a random time series with an unstructured cluster of data points tends to produce a high dimensional function f [21], the return maps of ON 5 through 7 in Figure 4 seem to indicate a relatively low value of L. It can also be inferred from Figure 4 that the function f is a nonlinear function [36].

The net heat release rate is determined using the usual heat release method [32], that applies the first law analysis on the engine charge assuming ideal gas properties. The heat release rate for sample operating point is shown in Figure 2. Heat release return maps for conditions corresponding to 5 operating conditions of Table 2 is shown in Figure 5. The experimental measurements are dispersed for ON 3 and 4 indicating the effects of stochastic component of measurements. By increasing the octane number, these fixed concentrated points start to destabilize in certain directions of the return map. The highest levels of destabilization occurs for cases of ON 6 and 7 in Figure 5.

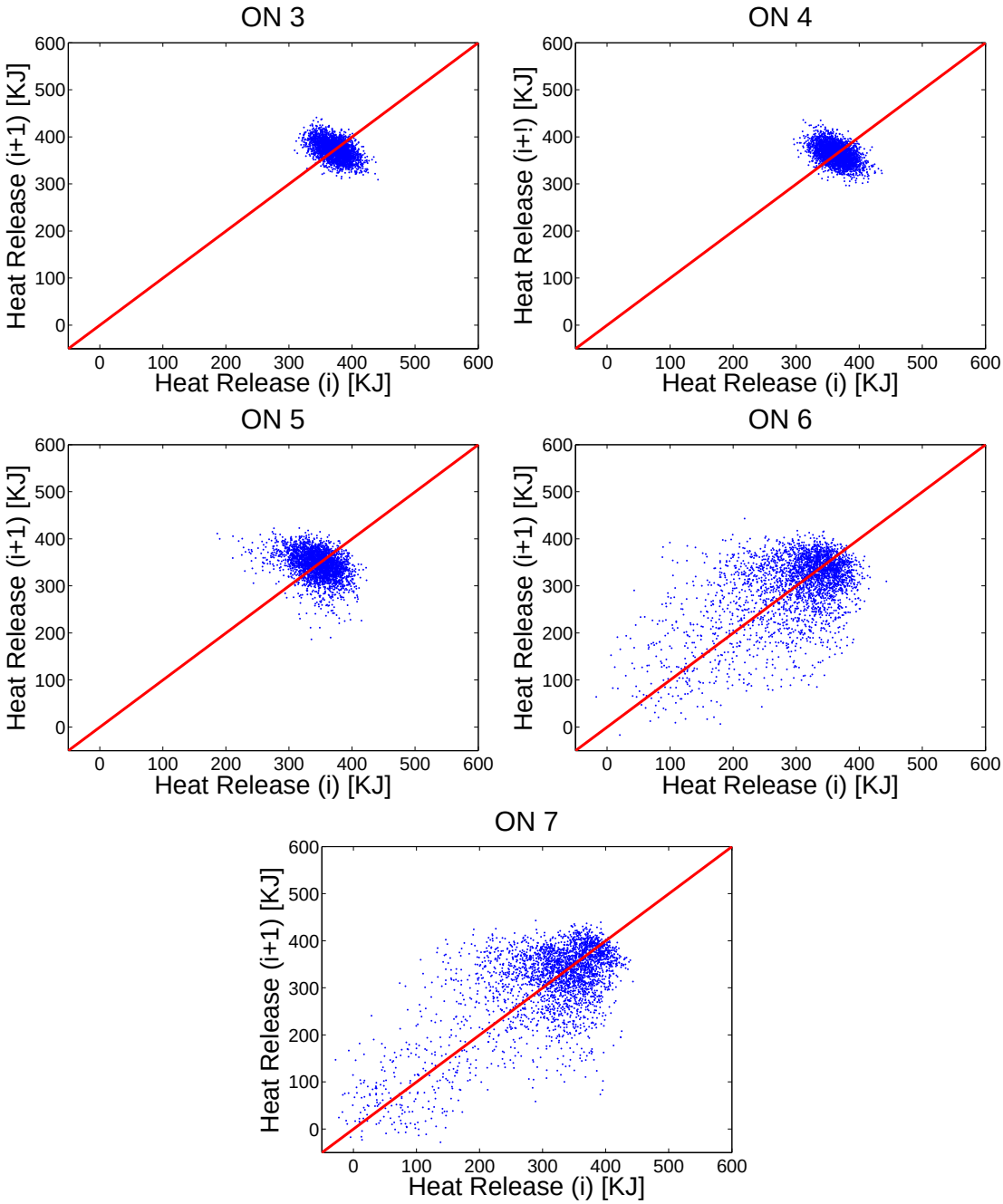

Figure 5: Return map of H.R. for 5 octane numbers. conditions listed in Table 2

3.2. Symbol-sequence Analysis

The symbol-sequence method is used to extract information from the experimental measurements of θ_{Pmax}. This method is used to detect the patterns occurring in the data points and is useful when dealing with data with high measurement error or dynamic noise [13]. Symbolization includes generating discretized symbols from raw experimental analog signals. The symbolization method is based on partitioning the original data points into

finite discrete regions and each region is then attributed to a particular symbolic value. The number of possible symbols n is called the symbol-set size [20, 37, 38]. This conversion has the practical effect of producing low-resolution data from high resolution data and reducing the effect of dynamic and measurement noise. In a practical sense for combustion timing prediction and control purposes in this work, the more qualitative description such as early or late combustion timing is desired. After symbolization, each group of symbols form a finite-length template called the symbol sequence L. The symbol sequence consists of consecutive symbols stepping through the whole data set point-by-point to form a new sequence. The sequence of symbols carries some important information about the experimental dynamics [16]. The total possible number of symbol sequences N is a combination of symbol-set size n and symbol sequence length L as follows: $N = n^L$ [16].

The symbol-sequence approach is used to detect inherent structure in experimental data despite a random-like appearance. This is performed by observing if some patterns dominant the time series, since a Gaussian process would on average have a flat histogram of the N symbol-set [13].

For the HCCI combustion data near misfire, θ_{Pmax} is partitioned equally in eight partitions, n=8, in a symbol series from 0 to 7. The data points, below the first bottom partition are assigned to symbol 0 and those between the first and second partition are assigned to symbol 1 and so on. The relatively high number of eight partitions is selected to extract detailed information from the original data set despite that the observed dynamics are obscured with noise [37, 39].

Much of the deterministic structure inherent in the data can be captured using the symbol-sequence approach [38]. A joint probability distribution to predict the next cycle occurrence using previous cycle information is used to determine L. These joint probability histograms give the maximum likelihood probability of next cycle given the occurrence of previous cycles in the whole time series. Then by comparing the one-cycle ahead predictions for different values of L, an optimal value of L can be determined. These histograms also give the probabilistic function for different data series. For the engine test points (with return maps in Figure 4), the optimal one-step ahead prediction is found using two previous cycles ($L = 2 + 1 = 3$).

Another important way to choose the optimum value of L is to employ Shannon entropy. Shannon entropy is a quantitative measure of nonrandom structure in time series measurements based on information theory. Because Shannon entropy provides an unambiguous indicator of temporal patterns, it is useful in determining the optimum sequence length L [38]. Shannon entropy is defined as:

$$H_S(L) = -\frac{1}{log(N)} \sum p_L log(p_L)$$

where N is the total number of symbol sequences with nonzero frequency, p_L is the probability of observing a sequence L. For the defined quantity, a value of one indicates the measured data are random, while a value of less than one indicates the presence of temporal correlation [40]. In the current context, lower H_S implies more deterministic structure. The value of H_S varies as the sequence length L changes. In this work, it is found that H_S typically reaches a minimum value as L is increased from 1. This trend is shown in Figure 6 for the five operating points listed in Table 2. The minimum H_S occurs at a sequence length

of 3 which is optimal for these cases and also reflects the symbol-sequence transformation which best distinguishes the data from a random sequence.

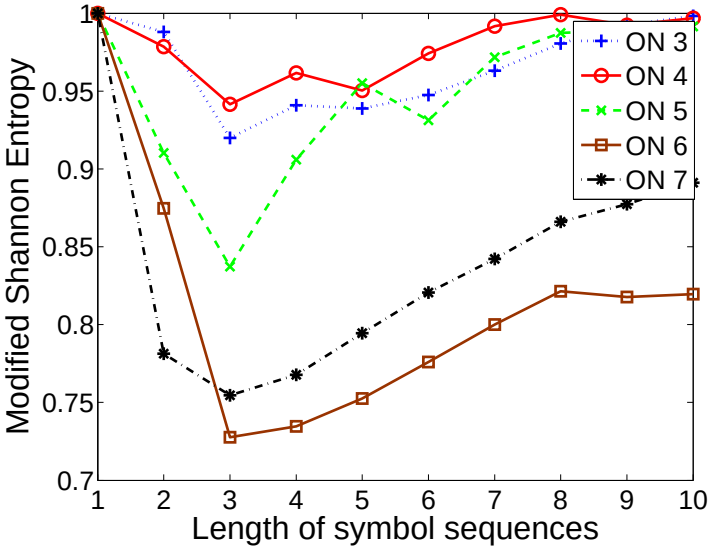

Figure 6: Modified Shannon entropy vs. symbol sequence length for 5 octane numbers. Conditions listed in Table 2

The symbol-sequence histogram for consecutive cycles of θ_{Pmax} corresponding to the data in Figure 4 is shown in Figure 7. In Figure 7, the vertical axis corresponds to the normalized frequency of occurrence of a symbol sequence and the horizontal axis is the symbol-sequence equivalent binary code. The symbol set size is $n = 8$ and sequence length is $L = 3$, resulting in $N = 8^3 = 512$ possible sequence codes.

A large normalized frequency peak accompanied by some smaller peaks in the sequence code histogram is apparent in the ON 7 plot of Figure 7 indicating a non-random sequence. The large peak occurs at sequence 0 (symbol series 000) which is three consecutive early values of θ_{Pmax} and physically corresponds to a weak combustion (most probably not having a main stage of combustion). Pattern number 438, which correspond to sequence 666, is also one of main local peaks for plots with ON 6 and ON 7. In addition, sequence codes 007 and 700, corresponding to pattern numbers 7 and 448 respectively, are among the possible sequences that the dynamics would pass through before entering or leaving three consecutive symbols of 0. For these cases, θ_{Pmax} does not stay in the late regions but oscillates between relatively early and late θ_{Pmax} angles. These local peaks indicate relative deterministic behavior of θ_{Pmax} combustion timing for the experimental cases with ON 6 and ON 7.

Symbol-sequence histograms are also useful for determining the time irreversibility since the relative frequencies will shift when analyzed with time reversal. It has been shown that an important method to discriminate the Gaussian random processes from deterministic prior-cycle effects is time irreversibility [41]. Particularly processes with non-random structure between consecutive cycles show an arrow of time which increases as the time dependence between cycles increases. On the other hand, processes with random inherent structure are symmetrical in time (i.e. the behavior of the forward and reverse time series are the same)

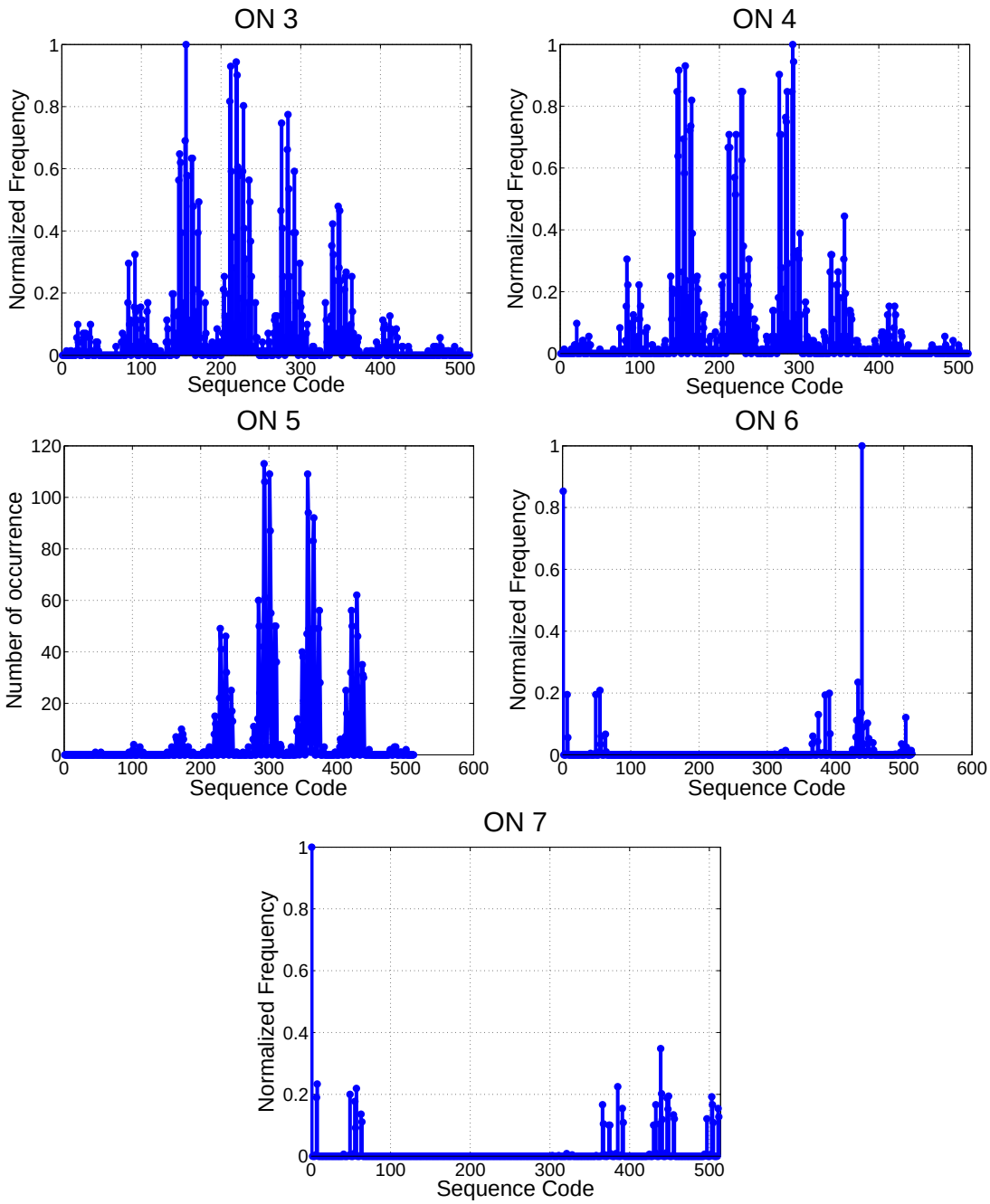

Figure 7: θ_{Pmax} symbol sequence histogram with (n=8, L=3) for HCCI combustion cycles 1 to 3000 (conditions as in Figure 4)

[11]. Time irreversibility versus the five cases is plotted in Figure 8 and shows that increasing the octane number results in higher time irreversibility. The details of time irreversibility for the operating points studied in this work are listed in the Appendix. The higher time irreversibility close to the engine misfire region at higher octane numbers is also an indication of having more deterministic patterns in that region. These deterministic patterns can be

captured in a chaotic predictive model and is detailed next.

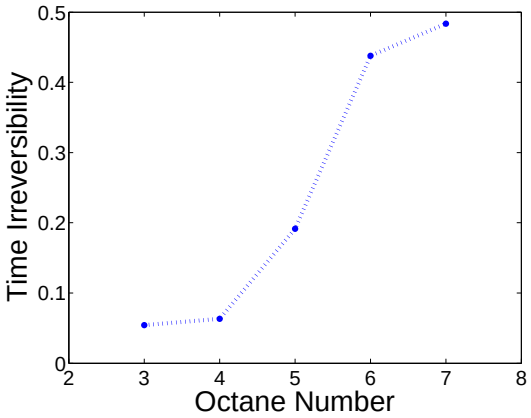

Figure 8: Time irreversibility versus octane number (conditions as in Figure 4)

3.2.1. Chaotic Predictive Model with Added Fuel Octane Number Dynamics

HCCI combustion timing is not only dependant on the temperature and pressure of the compression stroke, but also on the fuel chemistry and burnt gas residual from previous cycles [42]. The cycle-by-cycle combustion timing is strongly dependant on the octane number [43] which can be changed cycle-by-cycle in this experiment by injecting two fuels (n-heptane and iso-octane) using two fuel injectors. The fuel octane number can be used to increase the load range of the HCCI engine [44].

The range of HCCI combustion timing for each of the five octane numbers is shown in Figure 9. All other inputs are kept constant but the variation of θ_{Pmax} increases with increasing octane number as the engine has more misfire cycles. The combustion timing angle increases as expected with an increase in fuel octane number for octane numbers ranging between 3 to 5. By increasing the octane number further, the average θ_{Pmax} advances primarily due to θ_{Pmax} occurring early due to partial burn or misfire. The variation of θ_{Pmax} also increases with octane number due to the combustion instability.

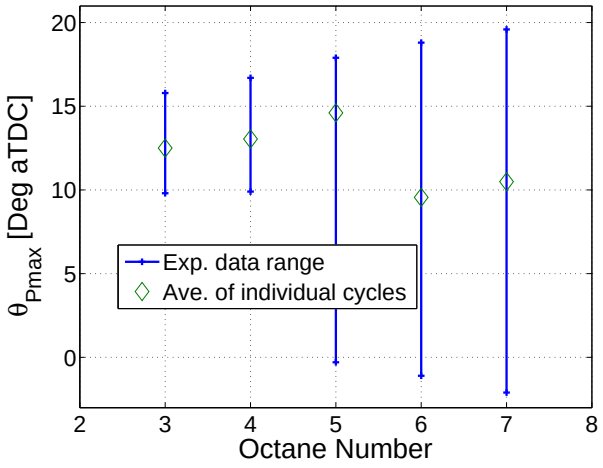

Figure 9: Combustion timing range of engine for 5 octane numbers used for HCCI combustion operating points near misfire (conditions as in Figure 4)

Nonlinear Prediction. A schematic of the real-time chaotic prediction for all five octane numbers is shown in Figure 10. To predict θ_{Pmax} with varying octane number, the interpolated deterministic part of the data captured by each of the five models is used. To obtain the predicted return map, the octane number and two previous θ_{Pmax} values are used to predict θ_{Pmax} of the next cycle such that the pattern of two previous inputs for each of the five octane numbers and the input octane number determines the most probable one step ahead θ_{Pmax}.

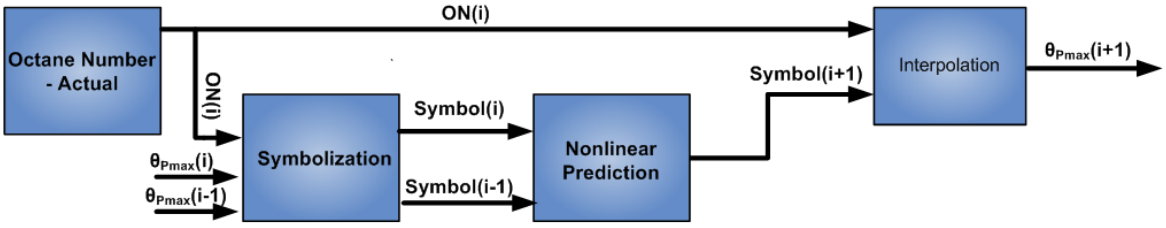

Figure 10: Schematic of the chaotic prediction used in Figure 14 for prediction of θ_{Pmax} for HCCI combustion operating points near misfire conditions

Using the joint probability estimator of θ_{Pmax} for each of the five operating points and the measured octane number in the test where the octane number varies between 3 to 7, the simulated behavior of consecutive cycles of θ_{Pmax} is constructed. To predict θ_{Pmax}, the following form is used:

$$\theta_{Pmax}(i) = f(ON(i), \theta_{Pmax}(i-1), \theta_{Pmax}(i-2), ..., \theta_{Pmax}(i-(L-1))) \quad (1)$$

The experimental data for θ_{Pmax} in Figure 11(a) is compared to the prediction for the same cycles in Figure 11(b). The direction of arrows in Figure 11(b) illustrates transitions between different θ_{Pmax} phase plane locations and gives an indication of the complexity of the dynamics.

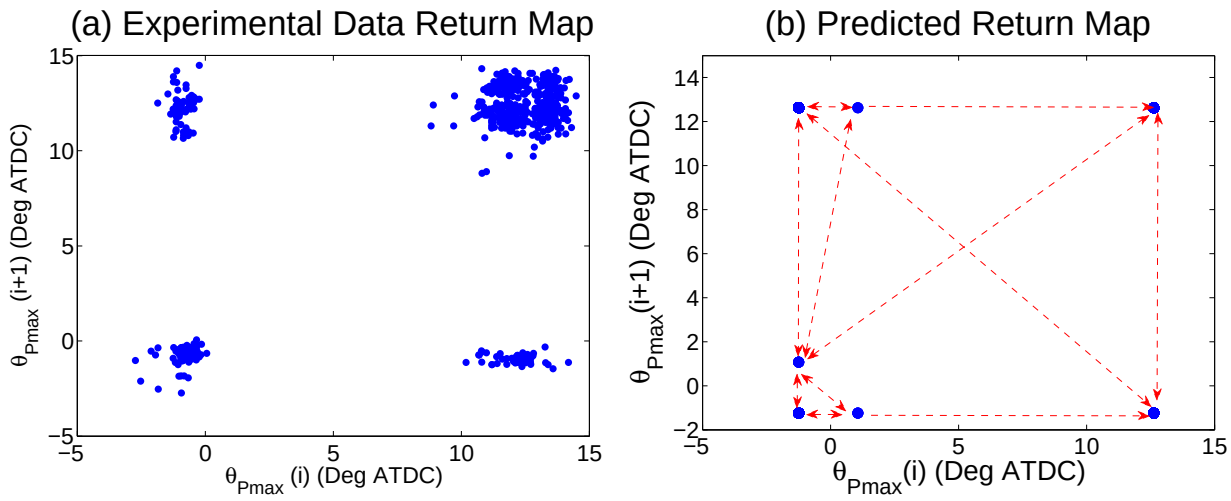

Figure 11: Comparison of experiment and prediction of θ_{Pmax} for HCCI combustion with varying octane number

The predicted return map in Figure 11(b) has the general appearance of the experimental data in Figure 11(a).

Prediction Validation. Cycles 900 to 1250, a 350 cycle portion of the test point with varying octane number, is used to check the prediction quality. The residual ($\Delta\theta_{Pmax} = \theta_{Pmax}(pred) - \theta_{Pmax}(measured)$) is shown in Figure 12 and autocorrelation of the residual is shown Figure 13.

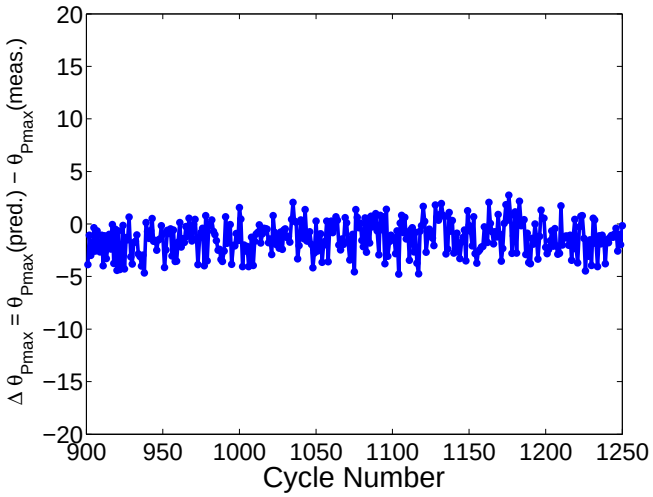

Figure 12: Prediction error ($\Delta\theta_{Pmax}$) between predicted values and experimental measurements for HCCI combustion (same condition as in Figure 11)

No obvious visible pattern in the residual error values in Figure 12 indicate, as a simple first check, that there is no dependency between consecutive error values and the model

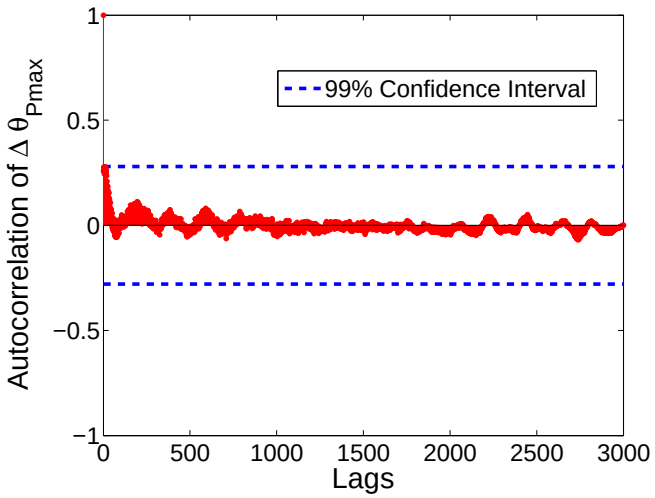

Figure 13: Autocorrelation of residuals ($\Delta\theta_{Pmax}$) for predicted consecutive cycles for HCCI combustion (same condition as in Figure 11)

seems to capture the dynamics. To further check this, the autocorrelation function for the residuals ($\Delta\theta_{Pmax}$) is shown in Figure 13 for all the 3000 $\Delta\theta_{Pmax}$ residuals. The 99% confidence interval is shown by dashed lines. Ideally for an acceptable model the correlation curves should fall between these lines [45] which is the case in Figure 13.

3.2.2. Controller

θ_{Pmax} control based on a chaotic predictive model using fuel octane changes. To control the unstable HCCI operating region, the fuel octane number is varied using two injectors. Iso-octane is injected by one injector while n-heptane is injected by the other and by varying the volumetric ratio the octane number in the engine can be changed cycle by cycle.

A proportional-integral (PI) controller using combustion timing for the next cycle as determined by the chaotic predictive model, regulates combustion timing (θ_{Pmax}) by varying the ration of iso-octane and n-heptane. A block diagram of the control system is shown in Figure 14. A single-input single-output controller is used since other inputs are kept constant. Since the engine combustion timing θ_{Pmax} can have a chaotic pattern, i.e. for an early/late θ_{Pmax} the next cycle could have late/early combustion timing, the chaotic predictive model described previously, is used to predict the next cycle combustion timing. This prediction is used as the feedback signal to stabilize the combustion timing.

To implement the control in real time, θ_{Pmax} is calculated from 0.1 degree cylinder pressure data at each cycle. This value θ_{Pmax}(i, i-1) in Figure 14 is output to the engine controller once per engine cycle and well before the next combustion. The engine controller is combustion event based with a sampling rate of once every two engine revolutions and modulates the two fuels to command the injector pulse widths to set the fuel octane (wall wetting is ignored) while maintaining a constant injected fuel energy despite changing the octane number.

The PI controller is tuned using simulation and then manually adjusted on the real engine. The controller implementation is $u_i = k_P e_i + k_I \sum e_j$ where $e = \Delta\theta_{Pmax}$ is the

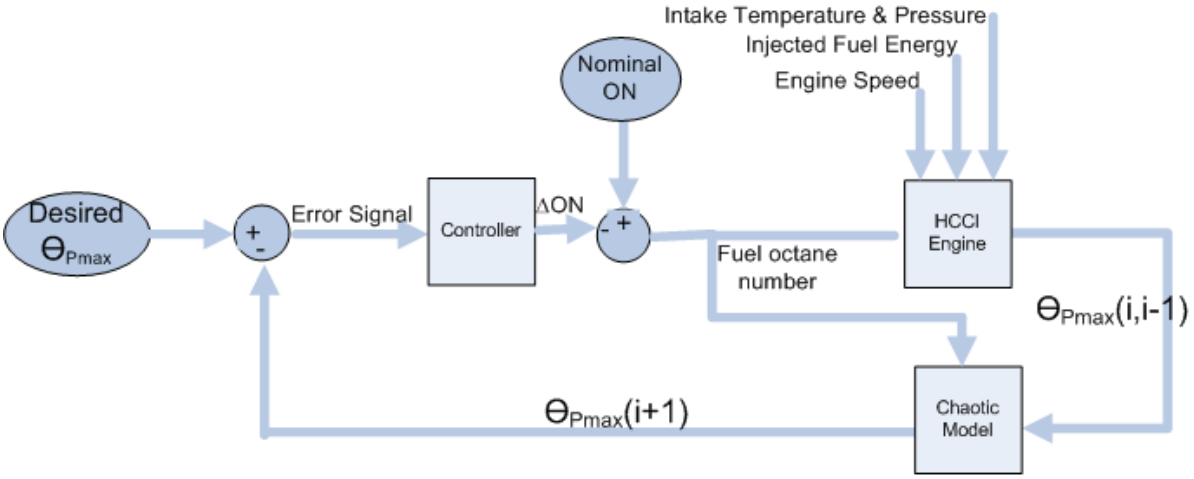

Figure 14: Schematic of the Controller of HCCI combustion timing for θ_{Pmax} in unstable region using fuel octane

difference between the desired and predicted θ_{Pmax}, and u is the controller output ΔON as shown in Figure 14.

Experimental Results. With PI control, the fuel octane number (input) and θ_{Pmax} (output) are recorded and shown in Figure 15. For this case θ_{Pmax} is about 10 °aTDC for normal combustion and 0 °for misfire. Cycles 800 to 900 show uncontrolled engine operation with the controller off and the octane number manually set to 5. At cycle 901, the PI controller is activated and modulates the octane number to stabilize θ_{Pmax} to the desired value. As seen in Figure 15, the controller reduces θ_{Pmax} variation resulting in a more stable engine operation with fewer misfire cycles. The average octane number is about 4 for the controlled portion of cycles 901 to 1260. The uncontrolled operation of the engine with the same conditions and octane number 4 exhibits unstable operation with misfire cycles as shown in Figure 16. The minor change in operating conditions (specifically intake manifold pressure) results in unstable operation of Figure 16 compared to conditions of Figure 4. The standard deviation of θ_{Pmax} decreases from 6.2 °(for cycles 800 to 900 without control) to 2.5 ° for the next 360 cycles with control. Most θ_{Pmax} values are within the normal operating condition of the engine after the controller is turned on although the control is not perfect with some cycles near misfire. This can be quantified by counting the percentage of misfire cycles for the region with the controller on (3%) versus percentage of misfire cycles for the uncontrolled operation (79%).

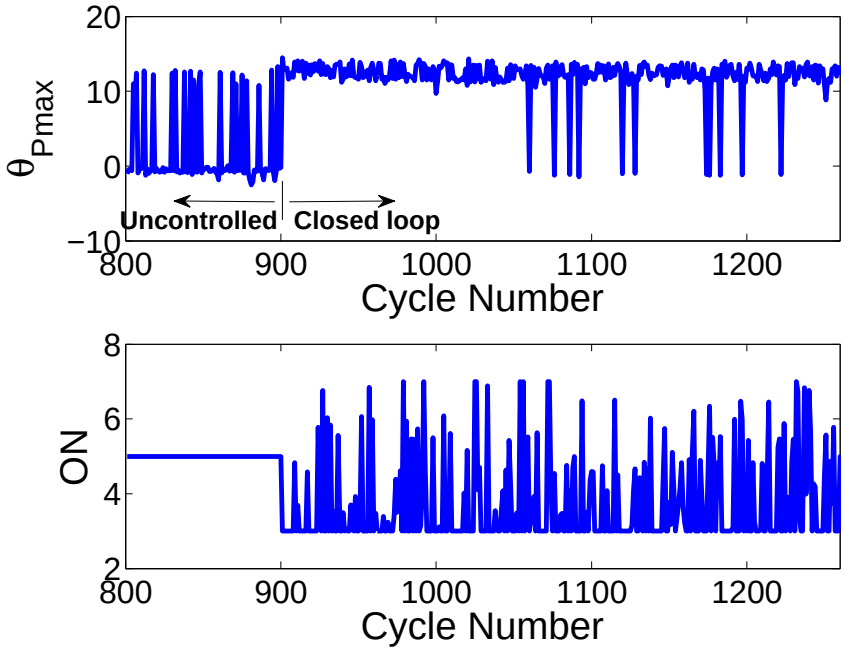

Figure 15: Combustion timing θ_{Pmax} using fuel octane input. Controller is turned on at cycle 901; $k_P = 1.7; k_I = 0.1$

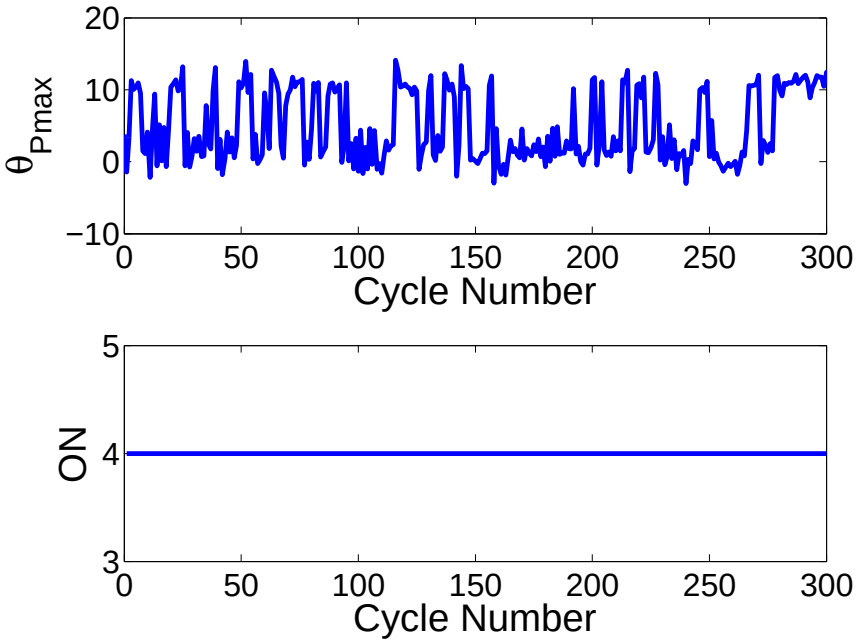

Figure 16: Combustion timing θ_{Pmax} using fuel octane input. Uncontrolled Operation

The pressure trace for the last two cycles of the uncontrolled operation (cycle 899 and 900) and the first two cycles of the controlled operation condition (cycle 901 and 902) are shown in Figure 17. Cycle 899 and 900 have the characteristics of misfire cycles while 901 and

902 have the characteristics of HCCI combustion indicating that the controller is effective.

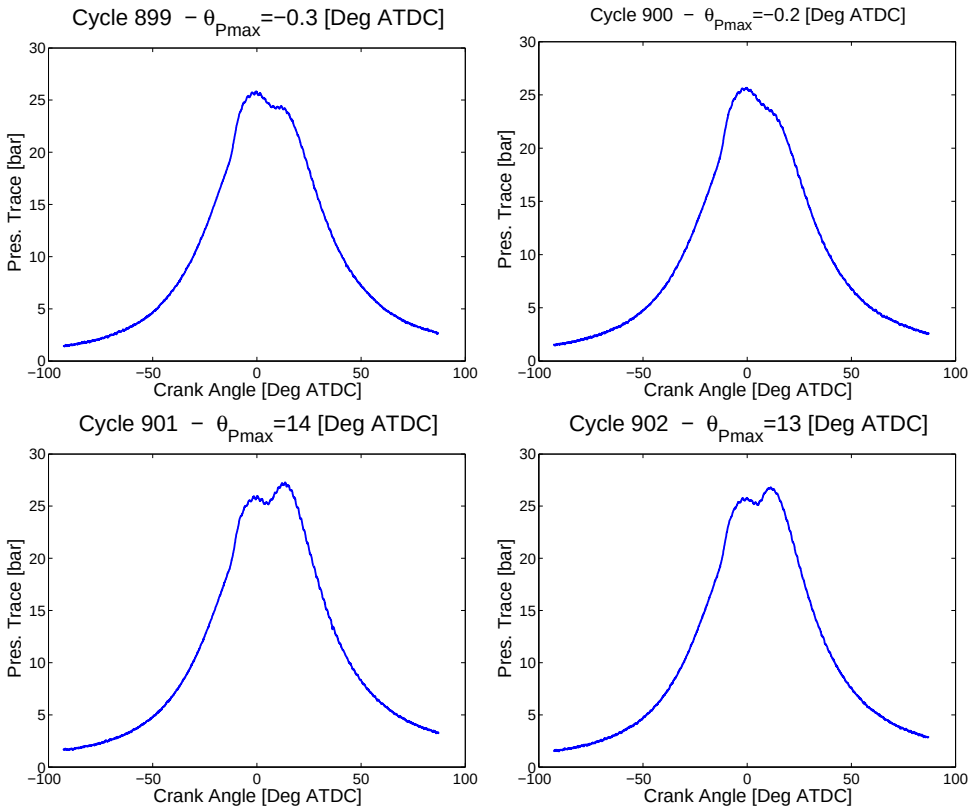

Figure 17: Cylinder pressure trace of cycles 899-902 of Figure 15

4. Conclusions

Deterministic patterns in cyclic variation of ignition timing (θ_{Pmax}) at operating points near the misfire limit of an HCCI engine are observed. Near the misfire limit the return map of θ_{Pmax} consists of multiple different regions, indicating non-constant nonlinear combustion timing. Non-random patterns of cyclic variation of ignition timing θ_{Pmax} under specific operating conditions emerge in symbol sequence analysis as large peaks in the symbol-sequence histogram and indicate a coupling between consecutive cycles. A joint probability estimator to predict one cycle ahead using the two previous cycles is developed and is used to predict combustion timing. An autocorrelation of predicted-actual θ_{Pmax} residual shows uncorrelated residuals which indicates that the joint probability model is acceptable. For the one base engine operating condition tested, θ_{Pmax} one cycle prediction is used to command fuel octane number (and thus modify combustion timing θ_{Pmax}) and results in a significantly lower number of misfires. The θ_{Pmax} prediction is combined with feedback control and demonstrates lower HCCI combustion variation and misfire rates in an experimental engine at one operating point for the same average octane number. This indicates that this method could potentially be used to extend into the misfire region of the HCCI engine range.

5. Acknowledgments

The authors acknowledge the Natural Sciences and Engineering Research Council of Canada (NSERC) and AUTO21 Network of Centers of Excellence for supporting this work. For his contributions in collecting the experimental data A. Audet [46] is gratefully acknowledged.

References

[1] R. Stanglmaier, C. Roberts, Homogeneous Charge Compression Ignition (HCCI): Benefits, compromises, and future engine applications, SAE Paper No. 1999-01-3682.

[2] H. Santoso, J. Matthews, W. K. Cheng, Managing SI/HCCI Dual-Mode Engine Operation, SAE Paper No. 2005-01-0162.

[3] M. Shahbakhti, C. R. Koch, Characterizing the Cyclic Variability of Ignition Timing in a Homogenous Charge Compression Ignition Engine Fueled with N-heptane/Iso-octane Blend Fuels, Int. J. Engine Res. 9 (2008) 361–397.

[4] E. Galloni, Analyses about Parameters that Affect Cyclic Variation in a Spark Ignition Engine, Applied Thermal Engineering 29 (2009) 1131–1137.

[5] C. Daw, C. Finney, M. Kennel, F. Connolly, Cycle-by-cycle Combustion Variations in Spark-Ignited Engines, Proceeding of the Fourth Experimental Chaos Conference Boca Raton, Florida.

[6] C. Daw, C. Finney, J. Green, A Simple Model for Cyclic Variations in a Spark-Ignition Engine, SAE Paper No. 962086.

[7] A. K. Sen and R. Longwic and G. Litak and K. Gorski, Analysis of Cycle-to-cycle Pressure Oscillations in a Diesel Engine, Mechanical Systems and Signal Processing 22 (2008) 362–373.

[8] M. Selik, R. Baraniuk, M. Haag, Signal Classifications and Properties, Tech. rep., Work produced by The Connexions Project and licensed under the Creative Commons Attribution License (2007).

[9] L. Guo-xiu, Y. Bao-feng, Nonlinear dynamics of cycle-to-cycle combustion variations in a lean-burn natural gas engine, Applied Thermal Engineering 28 (2008) 611–620.

[10] A. K. Sen and J. Zheng and Z. Huang, Dynamics of Cycle-to-cycle Variations in a Natural Gas Direct-Injection Spark-Ignition Engine, Applied Energy 88 (2011) 2324–2334.

[11] J. Green, C. Daw, J. Armfield, C. Finney, P. Durbetaki, Time Irreversibility of Cycle-by-Cycle Engine Combustion Variations, Proceeding of the 1998 Technical Meeting of the Central States Section of the Combustion Institue Lexington, Kentucky USA.

[12] R. K. Maurya and A. K. Agarwal, Experimental Investigation on the Effect of Intake Air Temperature and AirFuel Ratio on Cycle-to-cycle Variations of HCCI Combustion and Performance Parameters, Applied Energy 88 (2011) 1153–1163.

[13] R. Wagner, J. Drallmeier, C. Daw, Origins of Cyclic Dispersion Patterns in Spark Ignition Engines, Proceeding of the 1998 Technical Meeting of the Central States Section of the Combustion Institue Lexington, Kentucky USA (1998) 213–218.

[14] G. Litak and T. Kaminski and R. Rusinek and J. Czarnigowski and M. Wendeker, Patterns in the Combustion Process in a Spark Ignition Engine, Chaos, Solitons and Fractals 35 (2008) 578–585.

[15] M. Wendeker and J. Czarnigowski and G. Litak and K. Szabelski, Chaotic Combustion in Spark Ignition Engines, Chaos, Solitons and Fractals 18 (2003) 803–806.

[16] C. Daw, C. Finney, M. Kennel, A Symbolic Approach for Measuring Temporal Irreversibility, Phys. Rev. E 62(2) (2000) 1912–1921.

[17] C. Letellier, Symbolic Sequence Analysis Using Approximated Partition, Chaos, Solitons and Fractals 36 (2008) 32–41.

[18] B. Peter, Estimating and Improving the Signal-to-Noise Ratio of Time Series by Symbolic Dynamics, Phys. Rev. E 64 (2001) 051104.

[19] C. Daw, M. Kennel, C. Finney, F. Connolly, Observing and Modeling Nonlinear Dynamics in an Internal Combustion Engine, Phys. Rev. E 57 (1998) 2811–2819.

[20] C. Daw, C. Finney, E. Tracy, A Review of Symbolic Analysis of Experimental Data, Rev. of Sci. Instruments 74 (2003) 916–930.

[21] C. Daw, R. Wagner, K. Edwards, J. Green, Understanding the Transition Between Conventional Spark-Ignited Combustion and HCCI in a Gasoline Engine, 31st Int. Symp. on Proc. Combst. (Heidelberg, Germany; August 2006).

[22] A. Ghazimirsaied, M. Shahbakhti, C. Koch, HCCI Engine Combustion Phasing Prediction Using a Symbolic-Statistics Approach, J. Eng. for Gas Turbines and Power 132 (2010) 082805 1–5.

[23] C. S. Daw, K. D. Edwards, R. M. Wagner, J. B. Green, Modeling Cyclic Variability in Spark-Assisted HCCI, J. Eng. for Gas Turbines and Power 130 (2008) 052801.

[24] Yang, Dong-bo and Wang, Zhi and Wang, Jian-Xin and Shuai, Shi-jin, Experimental Study of Fuel Stratification for HCCI High Load Extension, Applied Energy 88 (9) (2011) 2949–2954.

[25] Machrafi, Hatim and Cavadias, Simeon and Amouroux, Jacques, A Parametric Study on the Emissions from an HCCI Alternative Combustion Engine Resulting from the Auto-Ignition of Primary Reference Fuels, Applied Energy 85 (8) (2008) 755–764.

[26] Komninos, N.P., Modeling HCCI Combustion: Modification of a Multi-Zone Model and Comparison to Experimental Results at Varying Boost Pressure, Applied Energy 86 (10) (2009) 2141–2151.

[27] Fathi, Morteza and Saray, R. Khoshbakhti and Checkel, M. David, The Influence of Exhaust Gas Recirculation (EGR) on Combustion and Emissions of N-heptane/Natural Gas Fueled Homogeneous Charge Compression Ignition (HCCI) Engines, Applied Energy In Press, Corrected Proof.

[28] Maurya, Rakesh Kumar and Agarwal, Avinash Kumar, Experimental Study of Combustion and Emission Characteristics of Ethanol Fuelled Port Injected Homogeneous Charge Compression Ignition (HCCI) Combustion Engine, Applied Energy 88 (4) (2011) 1169–1180.

[29] Gan, Suyin and Ng, Hoon Kiat and Pang, Kar Mun, Homogeneous Charge Compression Ignition (HCCI) Combustion: Implementation and Effects on Pollutants in Direct Injection Diesel Engines, Applied Energy 88 (3) (2011) 559–567.

[30] Komninos, N.P. and Kosmadakis, G.M., Heat Transfer in HCCI Multi-Zone Modeling: Validation of a New Wall Heat Flux Correlation Under Motoring Conditions, Applied Energy 88 (5) (2011) 1635–1648.

[31] Komninos, N.P., Investigating the Importance of Mass Transfer on the Formation of HCCI Engine Emissions using a Multi-Zone Model, Applied Energy 86 (7-8) (2008) 1335–1343.

[32] J. Heywood, Internal Combustion Engine Fundamentals, McGraw Hill, 1988.

[33] F. Matekunas, Modes and Measures of Cyclic Combustion Variability, SAE Paper No. 830337.

[34] U. Asad, M. Zheng, Fast heat release characterization of a diesel engine, J Thermal Sci. 47 (2008) 1688–1700.

[35] R. M. Wagner, C. S. Daw, J. B. Green, Characterizing Lean Spark Ignition Combustion Instability in Terms of a Low-Order Map, Proceeding of the 2nd Joint Meeting of the U.S. Sections of the Combustion Institue Oakland, California USA.

[36] R. Wagner, K. Edwards, C. Daw, J. J. Green, B. Bunting, On the Nature of Cyclic Dispersion in Spark Assisted HCCI Combustion, SAE Paper No. 2006-01-0418.

[37] X. Tang, E. Tracy, A. Boozer, A. Debrauw, R. Brown, Symbol Sequence Statistics in Noisy Chaotic Signal Reconstruction, Phys. Rev. E 51 (1995) 3871–3889.

[38] C. Finney, J. J. Green, C. Daw, Symbolic Time-Series Analysis of Engine Combustion Measurements, SAE Special Pub. 1330 (1998) 1–10.

[39] X. Tang, E. Tracy, R. Brown, Symbol Statistics and Spatio-Temporal Systems, Physica D 102: (1997) 253–261.

[40] R. Wagner, J. Drallmeier, C. Daw, Prior-Cycle Effects in Lean Spark Ignition Combustion - Fuel/Air Charge Considerations, SAE Special Publications (1998) 69–79.

[41] C. Diks, J. V. Houwelingen, F. Takens, J. Degoede, Reversibility as a criterion for discriminating time series, Physics Letters A 201 (1995) 221–228.

[42] G. T. Kalghatgi. Fuel Effects in CAI Gasoline Engines, HCCI and CAI Engines for the Automotive Industry, Chapter 9, Woodhead Publishing Limited, 2007.

[43] J.O. Olsson and P. Tunestal and B. Johansson, Closed-Loop Control of an HCCI Engine, SAE Paper No. 2001-01-1031.

[44] M. J. Atkins, C. R. Koch, The effect of fuel octane and diluent on HCCI combustion, Proc. IMechE Part D: J. Automobile Engineering 219 (2005) 665 – 675.

[45] NIST/SEMATECH e-Handbook of Statistical Methods http://www.itl.nist.gov/div898/handbook/ (Jan. 20, 2008).

[46] A. Audet, Closed Loop Control of HCCI Using Camshaft Phasing and Dual Fuels, Master's thesis, Univ. of Alberta (2008).

Appendix: Time-Irreversibility

The use of symbol-sequence histograms for determining the time irreversibility is used since the relative frequencies will shift when they will be observed with time reversed. It has been shown that one of most important features to discriminate the Gaussian random processes from deterministic prior-cycle effects is time irreversibility [41]. Particularly, processes with non-random structure between consecutive cycles show an arrow of time which increases as the nonlinear memory between cycles increase. On the other hand, processes with random inherent structure, is symmetric in time(i.e. the behavior of forward and reverse time series are the same) [11].

For the case when a process is time symmetric, there should not be a major difference between forward and backward time histogram. The observed relative frequency of the pattern numbers of a specific time series are compared with their reverse counterparts and the comparison is quantified with the following Euclidean-norm:

$$T_{irr} = \sqrt{\sum (F_i - R_i)^2} \tag{2}$$

where i is indexed over all possible sequence codes. F and R in the above equation are the histogram frequencies for the forward and reverse-time. The magnitude of T_{irr} is a quantitative measure of the level of time irreversibility. Figure 18 illustrates symbol-sequence histograms for the forward and reverse time of the HCCI θ_{Pmax} data corresponding to Figure 4. Reverse time series of the data points is generated by reversing the order of forward flow of data points.

In Figure 18 with ON 7, there are large peaks at sequence codes 0 (symbol sequence 000) and sequence code 438 (symbol sequence 666) for the forward direction which are very different in the reverse time realizations. This is attributed to the nonstationary or transient dynamics of the engine near the misfire limit, where the sequences of 0 or 6 occur often. The Euclidean-norm increases with octane number indicating that time irreversibility increases with increasing octane number as the engine operation approaches the misfire limit. As the engine is operated away from misfire (eventually knock could occur) the forward and reverse time symbol sequence histograms appear more similar to each other implying no major time irreversibility.

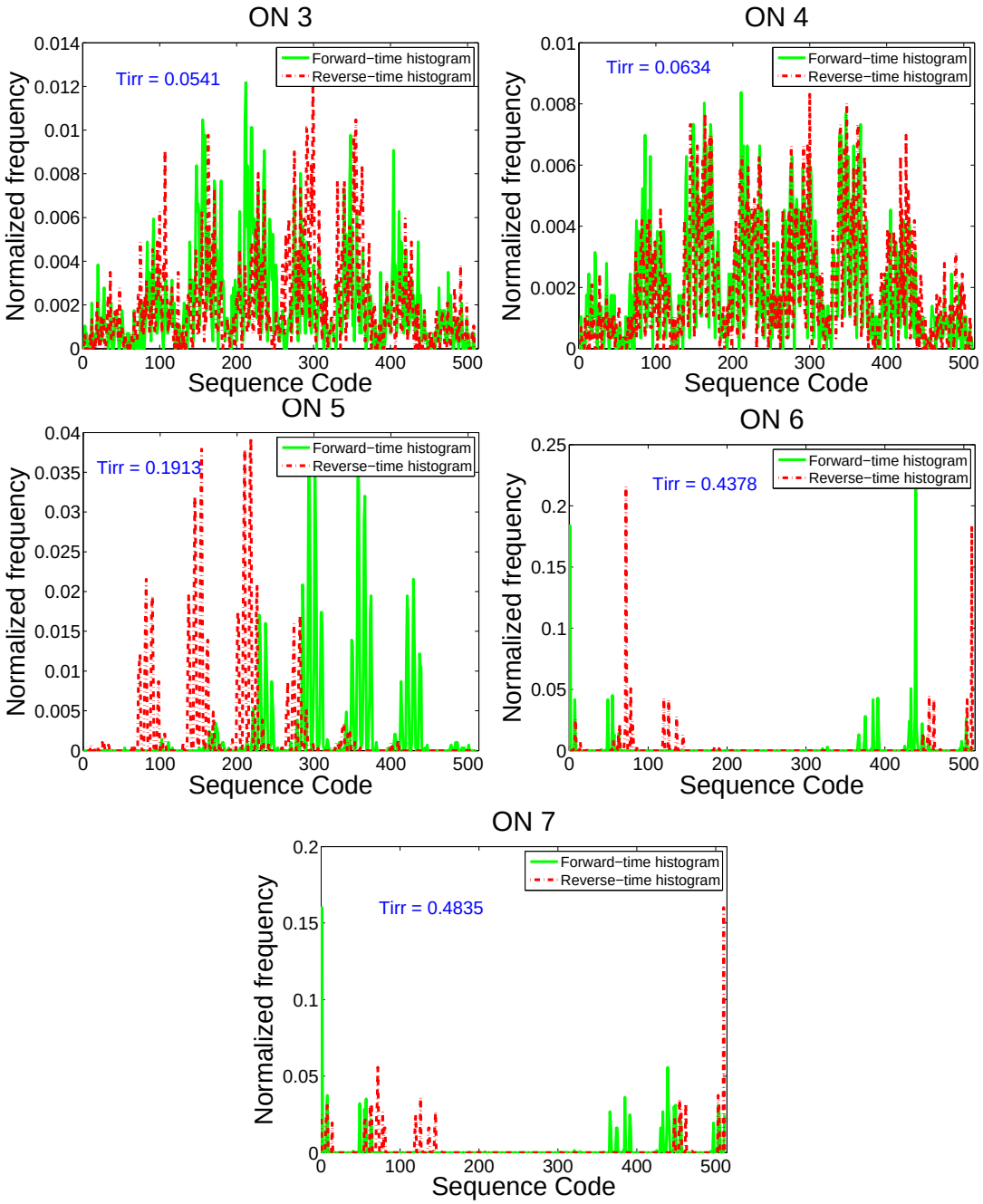

Figure 18: Forward and reverse θ_{Pmax} Symbol sequence histogram with (n=8, L=3) for HCCI combustion cycles 1 to 3000 (conditions as in Figure 4)

Appendix: Symbol Sequence Method

The principle idea of experimental data symbolization is to convert the time series values into a few possible values. Depending on the value of a given data, it is assigned to a symbolic value. The number of symbolic values is referred as the symbol-set size, which indicates the number of symbols available to symbolize the data; Figure 19 shows a portion of time series

of ignition timing for a sample point with conditions of ON 3 in Table 2. To illustrate the process the symbol-set size is selected as 2 and partition between symbols is located at the median of the data points. The data above the median is symbolized as 1 and the ones below the median as 0. The group of first consecutive three symbols, data points 1-3 form the symbol sequence 101, data points 2-4 form the sequence 011 and so on.

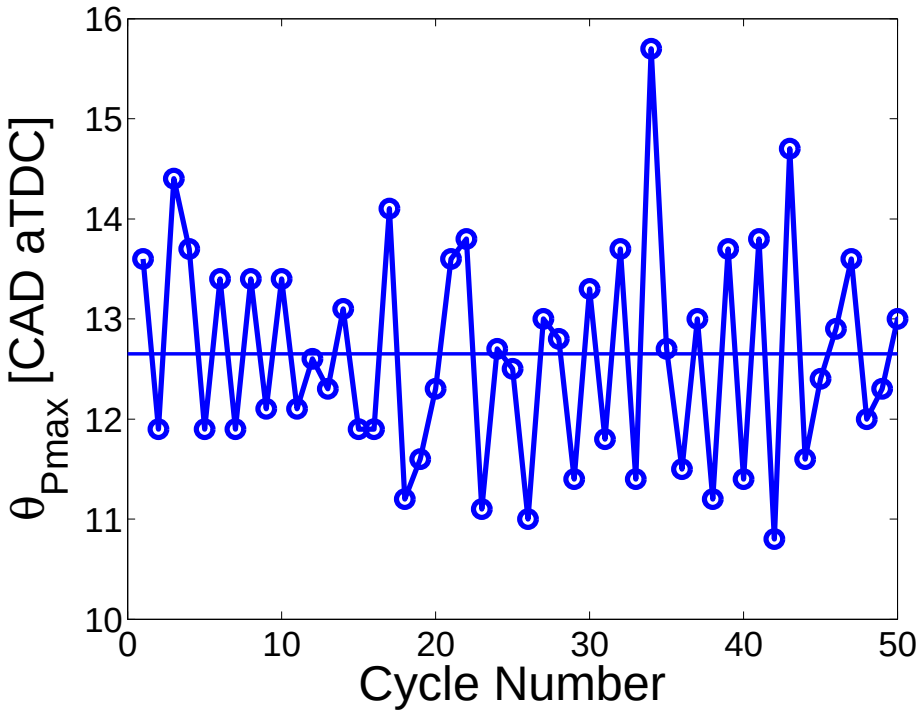

Figure 19: Ignition timing for a sample point with conditions of ON 3 of Table 2.

The symbol sequence histogram of Figure 19 is shown in Figure 20.

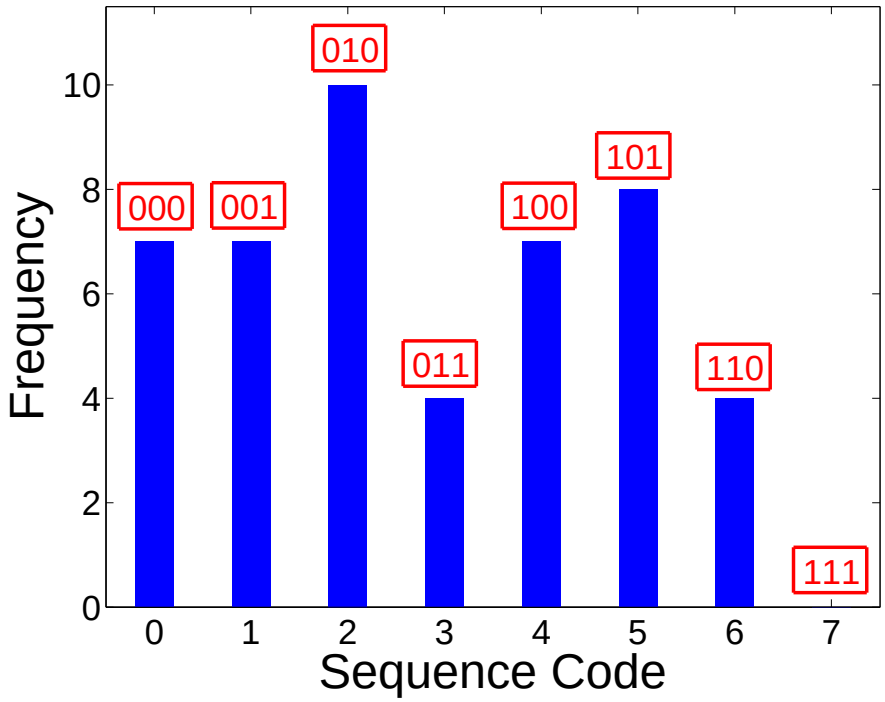

Figure 20: Ignition timing for a sample point with conditions of ON 3 of Table 2.

After data symbolization, the joint probability is calculated by counting the number of occurrence of each sequence. The resulting joint frequency histograms can be used to approximate the mapping function by determining the maximum likelihood estimate for the next cycle given the occurrence of a specific set of past cycles. An example of probability of occurrence of consecutive symbols is shown below:

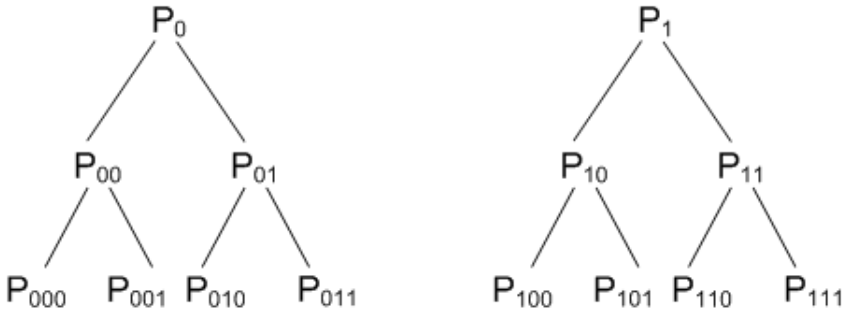

The probability of occurrence of three consecutive cycles P_{abc} emerges in the bottom level of the tree. The length of symbol sequence in this example is three which consists of three consecutive symbols. The sequence code is formed from converting the symbol sequences to their equivalent base-10 codes. For instance, in case of binary symbols used in this work, the symbol sequence 000 is equal to sequence code 0, 001 to 1, 010 to 2, 111 to 7 and so on. Symbol sequence histograms used in this paper are the representation of these symbol sequence probabilistic with the sequence codes as the horizontal axis values. A completely random time series results on average in equal frequencies for histogram with equal number and equiprobable sequence codes. Deterministic data sets show deviations from the equiprobability because of existing time correlations and dependency of data points.